

A FEASIBILITY STUDY FOR MULTI-MATERIAL RETROFITTABLE ENERGY ABSORBING STRUCTURE FOR AGED HELICOPTER SUBFLOOR.

R.Subbaramaiah^{1,2*}, G. Prusty¹, G.Pearce¹, S. H. Lim¹, D. Kelly¹, R. Thomson^{2,3}

1 School of Mechanical and Manufacturing Engineering,

University of New South Wales, Sydney, NSW, 2052, Australia

2 Cooperative Research Centre for Advanced Composite Structures,

506 Lorimer Street, Fishermans Bend, Victoria, 3207, Australia

3 Advanced Composite Structures Pty Ltd,

4/11 Sabre Drive, Port Melbourne, Victoria 3207, Australia

ravishankar.subbaramaiah@unsw.edu.au

Keywords: *Crashworthiness, Subfloor, Hybrid Material, Fibre Metal Laminate, Explicit FEA.*

Abstract

This paper outlines efforts to develop a retrofitable energy absorbing composite structure to metallic helicopter subfloors. It is envisaged to develop retrofitable structures using hybrid materials. A combination of metal and fibre reinforced composite layered structures are appropriate for this purpose as it not only enhances the crashworthiness but also minimizes issues like corrosion. The feasibility of layered aluminium and glass fibre reinforced composite hybrid structures are therefore being investigated for the development of reinforcement for helicopter subfloor members. Explicit finite element analysis tool like LS-DYNA and PAM-CRASH are used to model the crushing behaviour of these hybrid materials. In this paper the modelling strategies are discussed and the advantages of using hybrid materials are highlighted by comparing the mean crush force (kN) and specific energy of absorption (SEA). Designing such retrofits from hybrid composite increased crashworthiness can be attained with minimal penalty to structural weight and fewer complications than other retrofit solutions.

1 Introduction

The material share of composite has increased and is more than 50% in helicopters. An important requirement of the helicopter is energy absorbing capability of the subfloor.

Composite are extensively used these days in subfloors due to their high mass specific energy absorbing capability. The non-collapsible sub floor members are designed to provide a protective shell around the occupants. In a conventional subfloor structure [1, 2], the intersection elements shown in Fig. 1 are designed to absorb the main crash load and are the focus of the overall energy absorbing capability. Thus, the reinforcement of these elements becomes an important factor for improving the energy absorbing capability. Initial investigations were therefore made on the crushing of aluminium energy absorbing cruciform elements as shown in Fig. 1.

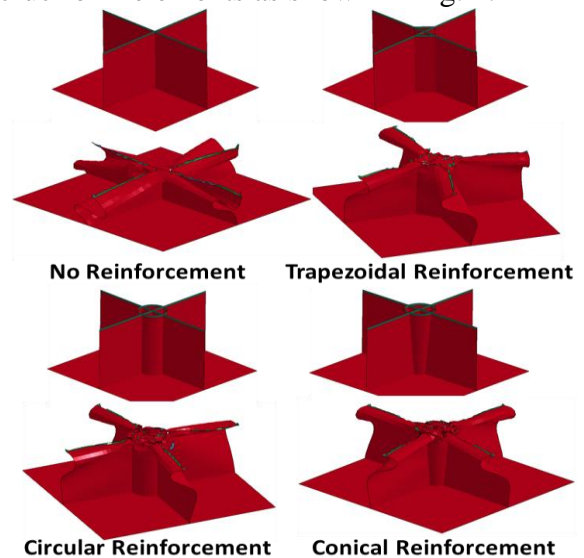


Fig. 1. Crushing Modes of subfloor intersections with metallic reinforcement.

In work carried out by McCarthy et al [3], Vignjevic[4] and Lanzi et al [5] new subfloor

design has been proposed with carbon fibre reinforced plastic (CFRP). It has been seen that composite cruciform elements have a more desirable SEA. The DLR Institute of Structures and Design has been constantly researching on the composite cruciform elements and advanced cruciform elements have been designed and tested by Johnson, Kindervater et al [6-8].

However material compatibility issues mean that it may not be advisable to use CFRP cruciform elements to reinforce aluminium subfloors of older helicopters. Glass fibre reinforced plastic (GFRP) have been demonstrated to be a superior choice of composite with aluminium in the studies done on composite wrapped aluminium tubes [9-12]. Hence in this paper GFRP and aluminium are investigated for use to form the hybrid material in designing retrofits to enhance crashworthiness of aluminium subfloors.

1.1 Crashworthiness

Among aluminium, GFRP and CFRP, CFRP composite materials are a strong candidate for the reinforcement material due to their excellent crashworthiness properties, specifically for their specific energy absorption (SEA) as shown in Fig. 2 CFRP has been used for crashworthiness in CRASURV [1] and wrapped aluminium/CFRP/GFRP crushing tubes [3, 4]

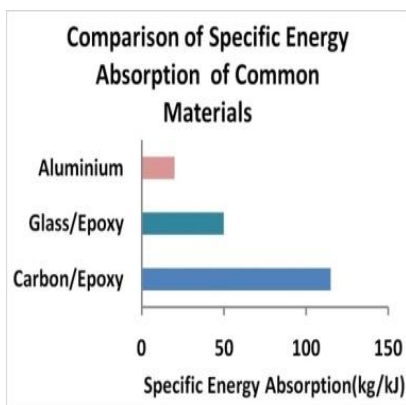


Fig. 2. Specific Energy Absorption.

However, due to their vastly differing material properties CFRP are not compatible with aluminium aircraft frames and their combination leads to corrosion and increased loading due to

thermal expansion and stiffness mismatch. This issue has led to Glass Fibre Reinforced Plastic (GFRP) being the preferred choice of the reinforcement material. Since the compatibility with aluminium is a major concern, an aluminium inclusive hybrid material, such as GLARE [5], becomes an appropriate choice and is worth investigating.

2 Explicit Finite Element Modelling

2.1 Quasi-static crush analysis of aluminium tube.

As an initial step in designing the hybrid material, square and circular tubes were quasi-statically crushed using numerical simulation.

LS-DYNA was used to build the explicit finite element analysis models. Two grades of aluminium tubes i.e., 2024-T3 and 6061-T6 were investigated with thickness of 1.4 mm of length 120 mm with 50 mm nominal diameter. LS-DYNA material model 18 [13] was used, it is an isotropic plasticity model with rate effects which uses a power law hardening rule, failure is based on plastic strain. The material properties are given in Table 1.

Aluminium Grade	2024-T3	6061-T6
Density (kg/mm ³)	2.77E-06	2.71E-06
Youngs Modulus (GPa)	7.31E+01	6.89E+01
Poisson's Ration	0.33	0.33
Yield stress. (GPa)	3.35E-01	2.91E-01
Plastic strain to failure	0.2578	0.3326

Table 1. Material properties of aluminium

A rigid plate of 100 kg is used to crush the aluminium tube with a constant velocity curve of 0.1 mm/s. A single surface automatic contact (ASSC) is defined for the metallic tube and a rigid wall is defined with the all the tube nodes as slave. The tube is constrained at the lower end using single point constraints (SPC). The mesh size of 2.5 mm * 2.5 mm is used for shell elements with Belytschko-Tsay formulation. A chamfer of 60° is used as a trigger.

The crush force and crushing mode for metal depends on various factors like trigger, tube

thickness, diameter, length, t/D ratio and cross sectional shape as listed in Fig. 9.

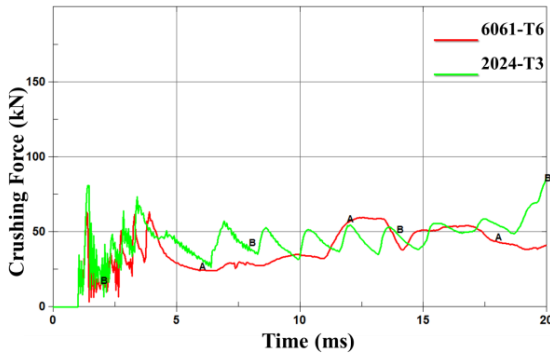


Fig. 3. Crushing Force of aluminium grades 2024-T3 and 6061-T6

As shown in Fig. 3 the predicted mean crushing force for 2024-T3 and 6061-T6 are 30 kN and 28.6 kN respectively. The crushing modes are shown in Fig. 4, 2024-T3 crushes with concertina mode and 6061-T6 is seen to have a diamond crushing mode. The mean crushing force is calculated by dividing the internal energy at a given stroke length divided by the stroke as given in equation 1.



Fig. 4. Crushing modes of aluminium tube.

$$Crushing\ Force_{\text{mean}} = \frac{Energy_{\text{internal}} @ L\text{mm}}{L} \quad (1)$$

The mean crushing force in Alexander [14] and Abramowicz [15, 16] were used to validate the model.

Grade	Yield Stress (MPa)	Mean Crushing Force (kN)		
		Alexander Model	Abramowicz Model	FEA
2024-T3	335	20.43	26.75	30.0
6061-T6	291	17.74	23.24	28.6

Table 2. Analytical and Numerical comparison of F_{mean} of aluminium grades.

A good comparison between mean crushing force estimated by FEA and Abramowicz model is seen in Table 2.

2.2 Quasi-static crush analysis of composite tube.

Quasi-static crushing of composite tubes of type carbon fibre/BMI resin and E-glass/epoxy were simulated using Mat54 [13] in LS-DYNA which is an enhanced composite damage model.

The failure criteria due to Chang-Chang is a modified version of the Hashin criterion. Here tensile and compressive fibre and matrix failure are separately considered. Normally both the strength and the stiffness are set equal to zero after failure is encountered. SLIMx terms can be used to reduce strength to a minimum value after maximum stresses are reached. In addition the layer in the element is completely removed after the maximum tensile or compressive strain in the fibre direction is reached.

The FEA model is setup similar to aluminium tube previously discussed. The material properties of the individual composite are given in Table 3. The fibres in the composite are at 90° to the tube axis, this is defined using the beta parameter in the *SHELL card. The crush force and crushing mode for composite depends on fibre stacking sequence, orientation, form (unidirectional/mat/fabric) as listed in Fig. 9.

Property	Description	Carbon	Glass
ρ (g/cm ³)	Density	1.53	1.80
Ea (GPa)	Longitudinal modulus (fibre direction)	135	30.9
Eb (GPa)	Transverse modulus (perpendicular to fibre)	9.12	8.3
Gab (GPa)	In-plane shear modulus (ab plane)	5.67	2.8
ν_{ba}	Minor Poisson's ratio	0.021	0.0866
Xt (MPa)	Longitudinal tension strength (fibre direction)	2326	798
Xc (MPa)	Longitudinal compressive strength (fibre direction)	1236	480
Yt (MPa)	Transverse tension strength (perpendicular to fibre)	51	40
Yc (MPa)	Transverse compressive strength (perpendicular to fibre)	209	140
Sc (MPa)	In-plane shear strength	87.9	70
DFAILT	Maximum strain for fibre tension	3%	2.3 %
DFAILC	Maximum strain for fibre compression	6%	1.4 %

Table 3. Material properties of carbon/BMI resin and E-glass/epoxy [10, 12].

The mean crush force of GFRP and CFRP are 11.4 kN and 13.6 kN respectively, their crushing force is shown in Fig. 5. As previous indicated in Fig. 2 the SEA of CFRP is 41.5 kJ/kg which is higher than that of GFRP 29.1 kJ/kg.

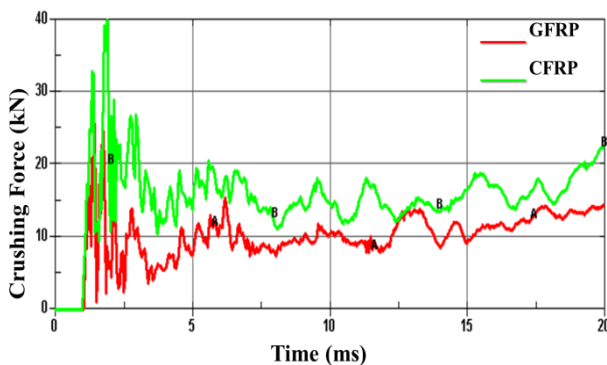


Fig. 5. Crushing force of GFRP and CFRP.

The crushing mode of the two composite with fibre in 90° are shown in Fig. 6 and Fig. 8.

The uncrushed tube, the crush initiation and fully crushed tube are shown in the front and top view.



Fig. 6. Crushing mode of GFRP.

It can be seen that the crushing modes of the glass/epoxy composite with fibre in 90° closely match the crushing modes reported in the experimental work in Fig. 7 [18].



Fig. 7.- Experimental crushing of glass/epoxy.



Fig. 8.- Crushing mode of CFRP

2.3 Crashworthiness of Hybrid Material.

Using the validated models, a tube is modelled with hybrid material with aluminium 2024-T3 and E-glass/epoxy. A layered shell

methodology is used to model the hybrid tube, the inner aluminium tube has an external diameter of 50 mm and thickness of 1.4 mm, the glass/epoxy layer is wrapped over the metallic tube and has a thickness of 1.4 mm. A 60° Chamfer is modelled as trigger. Belytschko-Tsay quadrilateral shell elements are used to model both layer with element size 2 mm. The fibres in the composite layer are at 90° orientation (hoop wrap). The tube is constrained at its lower end and a rigid wall is used to crush from the top.

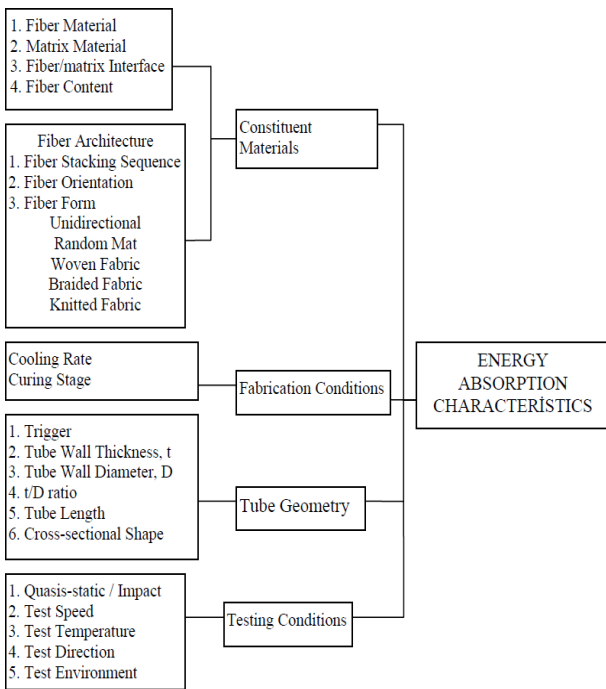


Fig. 9. Factors that influence energy absorption [17].

Contacts are defined to represent the bond between the two materials and avoid interpenetration as follows:

- CASST (Contact Automatic Surface to Surface Tie) is used to represent the bond between composite overwrap and aluminium tube. After failure, this contact option behaves as a surface-to-surface contact. The failure criterion has normal failure stress and shear failure stress governed by equation 2.

$$\left(\frac{|\sigma_n|}{NFLS}\right)^2 + \left(\frac{|\sigma_s|}{SFLS}\right)^2 \geq 1 \quad (2)$$

- CASS (Contact Automatic Single Surface) to prevent any interpenetration among folds, $\mu = 0.3$.
- A rigid wall of type Rigid Flat Motion is defined with all nodes considered to be slave nodes.

The failure equation 3 to equation 6 selected is based on the Chang-Chang criterion. Four indicator functions e_f , e_c , e_m , e_d , correspond to the four failure modes. These failure indicators are based on total lamina failure hypothesis, here both the strength and the stiffness are set equal to zero after failure is encountered.

For the tensile fibre mode (where “a” is fibre direction and “b” is transverse):

$$\sigma_{aa} > 0 \text{ then } e_f^2 = \left(\frac{\sigma_{aa}}{X_t}\right)^2 + \beta \left(\frac{\sigma_{ab}}{S_c}\right)^2 - 1 \begin{cases} \geq 0 & \text{failed} \\ < 0 & \text{elastic} \end{cases} \quad (3)$$

For the compressive fibre mode:

$$\sigma_{aa} < 0 \text{ then } e_c^2 = \left(\frac{\sigma_{aa}}{X_c}\right)^2 - 1 \begin{cases} \geq 0 & \text{failed} \\ < 0 & \text{elastic} \end{cases} \quad (4)$$

For the tensile matrix mode:

$$\sigma_{bb} > 0 \text{ then } e_m^2 = \left(\frac{\sigma_{bb}}{Y_t}\right)^2 + \left(\frac{\sigma_{ab}}{S_c}\right)^2 - 1 \begin{cases} \geq 0 & \text{failed} \\ < 0 & \text{elastic} \end{cases} \quad (5)$$

For the compressive matrix mode:

$$e_d^2 = \left(\frac{\sigma_{bb}}{2S_c}\right)^2 + \left[\left(\frac{Y_c}{2S_c}\right)^2 - 1\right] \frac{\sigma_{bb}}{Y_c} + \left(\frac{\sigma_{ab}}{S_c}\right)^2 - 1 \begin{cases} \geq 0 & \text{failed} \\ < 0 & \text{elastic} \end{cases} \quad (6)$$

In addition maximum strain limits are specified for fibre tension and fibre compression using DFAILT and DFAILC parameters in the Material Model 54 property card. Another parameter TFAIL, was used to set the time step quotient for element deletion. Starting with Version 971 Release R5 in material model 54 five SLIMx terms are included in the material card, these factors determine the minimum stress limit after stress maximum in the fibre and matrix in tension, compression and shear. The stress limits are factors used to limit the stress in the softening part to a given value as indicated by equation 7,

$$\sigma_{min} = SLIMx * strength \tag{7}$$

This is graphically shown in Fig. 10 in comparison to various other composite material models available in LS-DYNA.

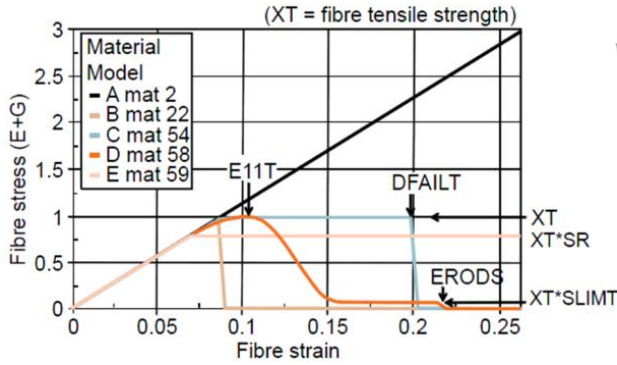


Fig. 10. Composite material models in LS-DYNA [19].

Additional measures are taken to delete elements which are highly distorted using the NFAIL parameter in the *Control card. The impact force is extracted by estimating the reaction force at the fixed end of the tube. Typical crushing modes of hybrid materials [12] are shown in Fig. 12.

In Fig. 11 it can be seen that the crushing modes of hybrid material are of type compound diamond with fibre orientation in 90°.

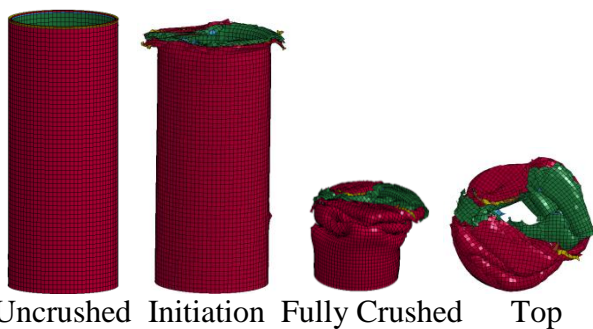


Fig. 11. Crushing mode of hybrid material.

The advantages of hybrid material such as aluminium and E-glass/epoxy can be seen in Fig. 13 with higher mean crushing force compared to its individual constituents E-glass/epoxy and aluminium 2024-T3.

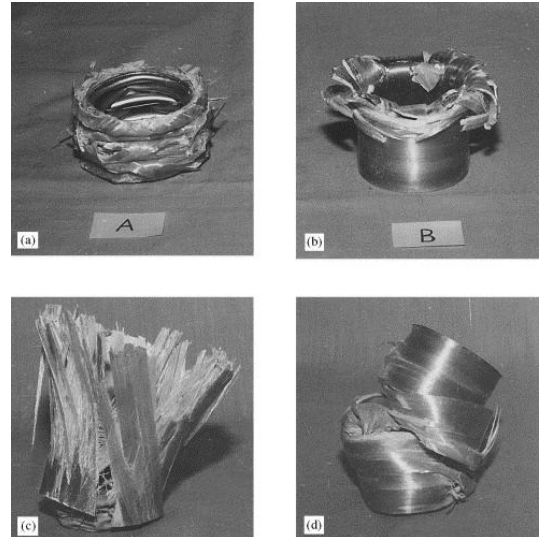


Fig. 12. Experimental crushing modes 9a) compound diamond, (b) compound fragmentation, (c) delamination, (d) catastrophic failure [12].

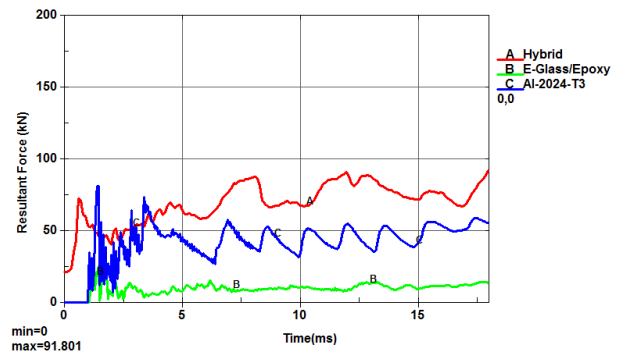


Fig. 13. Comparison of crushing force of aluminium, E-glass/epoxy and hybrid.

Hanefi et al [16] proposed a simplified analytical model for static crushing of externally reinforced metal tubes. The mean crush load is given by equation 8

$$4HP_m = 2\pi^2 a \sigma_0 C t_m^2 + 4\pi \left(\sigma_0 t_m + \frac{1}{2} \sigma_{cf} t_c \right) H^2 + \frac{2\pi a t_c E_c \epsilon_{ct}^2 H}{\tag{8}}$$

where ϵ_{ct} = Critical Strain, E_c = Young's Modulus, σ_{cf} = Yield Stress of composite, H = Half Folding length, t_c, t_m, a are geometric parameters of tube.

The Hanefi model was refined by Song [12] for hybrid tubes. Though these models were able to predict the mean crushing load accurately, there are certain drawbacks as the proposed model

holds good only for composite wrap with fibre orientation at 90° and for single layer.

Material	Mean Crushing Force (kN)	
	Hanefi Model	FEA
E-Glass/Epoxy Aluminium Hybrid.	45.53	54.30

Table 4. Comparison of Analytical and Numerical Mean Crushing force for hybrid material.

The FEA results compare well with the mean crushing force of hybrid tube as estimated by the Hanefi model as shown in Table 4.

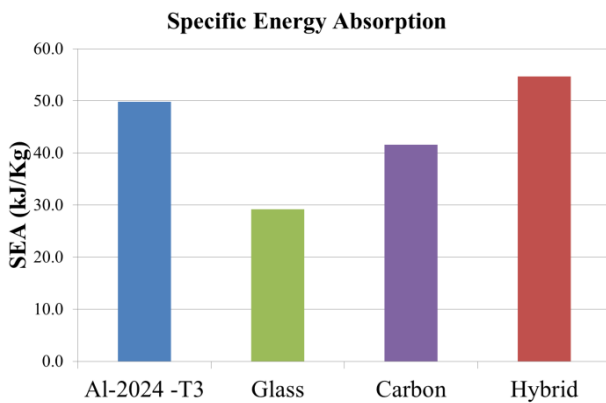


Fig. 14. Specific Energy of Absorption estimate through explicit FEA.

However the SEA of hybrid material shown in Fig. 14 is higher than that of the composite but is only marginally higher than the constituting aluminium layer.

3 Future work

The benefit of metal-composite hybrid material combination are shown in Fig. 13 and Fig. 14 will be extended to design the retrofit with thinner metallic layer to achieve higher SEA. The stack shell modelling approach will be extended to incorporate more layers of composite to predict crushing force more accurately.

3.1 Methodology and Approach

Methodology to design, analyse and verify the retrofit is outlined in Fig. 15. The design parameter critical to performance are number of layers, the fibre orientation in the composite layer and the individual layer thicknesses. A sustained progressive crushing has to be achieved to have an efficiently working energy absorbing system. This will be investigated by designing various design alternatives which are in form of conical, trapezoidal and cylindrically shaped retrofits.

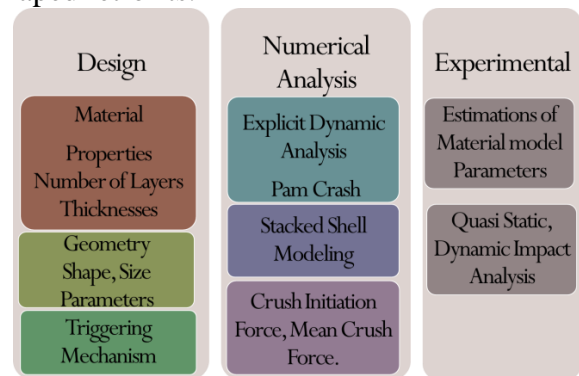


Fig. 15. Design Methodology

3.2 Design and Analysis of Subfloor intersection reinforcement.

A building block approach will be used to develop the retrofitable energy absorbing member to enhance the crashworthiness of the subfloor of rotorcraft. Experimental tests would be carried out at various phases of the design validation. Experiments for material characterisation would also be carried out and these would include extracting properties in order to define failure criteria for the hybrid tube.

4 Conclusion

It is seen that the hybrid material under quasi-static crushing has superior performance when compared to its individual constituents and can be adopted for the design of retrofit to enhance crashworthiness. The hybrid material retrofits can also be envisaged for retrofication in areas like airframes, seats and under-carriage for enhancing crashworthiness. Achieving low

manufacturing cost and the restricted formability of hybrid material are few challenges in designing these retrofits.

Overall the benefits of the retrofication will not only lead to enhancement of crashworthiness of aged helicopters but also increase its service life. By designing such retrofits from hybrid composite materials, increased crashworthiness can be attained with minimal penalty to structural weight and fewer complications than traditional retrofit solutions.

Copyright Statement

The authors confirm that they, and/or their company or organization, hold copyright on all of the original material included in this paper. The authors also confirm that they have obtained permission, from the copyright holder of any third party material included in this paper, to publish it as part of their paper. The authors confirm that they give permission, or have obtained permission from the copyright holder of this paper, for the publication and distribution of this paper as part of the ICAS2012 proceedings or as individual off-prints from the proceedings.

References

- [1] C. Bisagni. Energy absorption of riveted structures. *International Journal of Crashworthiness*, Vol. 4, pp 199 - 212, 1999.
- [2] C. Bisagni. Crashworthiness of helicopter subfloor structures. *International Journal of Impact Engineering*, Vol. 27, pp. 1067-1082, 2002.
- [3] M. A. McCarthy, C. G. Harte, J. F. M. Wigenraad, A. L. P. J. Michielsen, D. Kohlgrüber, and A. Kamoulakos. Finite element modelling of crash response of composite aerospace sub-floor structures. *Computational Mechanics*, Vol. 26, pp. 250-258, 2000.
- [4] R. Vignjevic and M. Meo. A new concept for a helicopter sub-floor structure crashworthy in impacts on water and rigid surfaces. *International Journal of Crashworthiness*, 2010.
- [5] L. M. Lanzi, C. Castelleti. Crashworthiness shape optimization of helicopter subfloor. *ICAS*, 2004.
- [6] A. F. Johnson, C. M. Kindervater, and K. E. Jackson. Multifunctional design concepts for energy absorbing composite fuselage sub-structures. *American Helicopter Society 53rd Annual Forum*, Virginia Beach, VA, USA, pp. 1115-1128, 1997.
- [7] C. M. Kindervater, A. F. Johnson, D. Kohlgrüber, M. Lützenburger, and N. Pentecote. Crash and impact simulation of aircraft structures - hybrid and FE based approaches. *European Congress on Computational Methods in Applied Sciences and Engineering*, Barcelona, Spain, 2000.
- [8] C. M. Kindervater, D. Kohlgruber, and A. Johnson. Composite vehicle structural crashworthiness - A status of design methodology and numerical simulation techniques. *International Journal of Crashworthiness*, Vol. 4, pp. 213 - 230, 1999.
- [9] J. Bouchet, E. Jacquelin, and P. Hamelin. Static and dynamic behaviour of combined composite aluminium tube for automotive applications. *Composites Science and Technology*, 2000.
- [10] H. El-Hage, P. K. Mallick, and N. Zamani. A numerical study on the quasi-static axial crush characteristics of square aluminium tubes with chamfering and other triggering mechanisms. *International Journal of Crashworthiness*, Vol. 10, pp. 183-195, 2005.
- [11] J. Bouchet, E. Jacquelin, and P. Hamelin. Static and dynamic behaviour of combined composite aluminium tube for automotive applications. *Composites Science and Technology*, Vol. 60, pp. 1891-1900, 2000.
- [12] H.-W. Song, Z.-M. Wan, Z.-M. Xie, and X.-W. Du. Axial impact behaviour and energy absorption efficiency of composite wrapped metal tubes. *International Journal of Impact Engineering*, Vol. 24, pp. 385-401, 2000.
- [13] *LS-DYNA keyword user's manual*, Version 971. Vol. I and II, 2012.
- [14] J. M. Alexander. An approximate analysis of the collapse of thin cylindrical shells under axial loading. *The Quarterly Journal of Mechanics and Applied Mathematics*, Vol. 13, pp. 10-15, 1960.
- [15] W. Abramowicz and N. Jones. Dynamic axial crushing of circular tubes. *International Journal of Impact Engineering*, Vol. 2, pp. 263-281, 1984.
- [16] E. H. Hanefi and T. Wierzbicki. Axial resistance and energy absorption of externally reinforced metal tubes. *Composites Part B: Engineering*, Vol. 27, pp. 387-394, 1996.
- [17] H. Hamada and S. Ramakrishna. Energy absorption characteristics of crash worthy structural composite materials. *Engineering Materials*, Vol. 141-143, pp. 585-620, 1998.
- [18] H. S. S. Aljibori. Energy absorption characteristics and crashing parameters of filament glass fibre /epoxy composite tubes. *European Journal of Scientific Research*, Vol.39, pp. 111-121, 2010.
- [19] R. Matheis. Numerical simulation of the crash behaviour of braided composites. *CFK-Valley Stade Convention*, 2011.